2011-01-07

High Power, Low Frequency Ultrasound: Meniscal Tissue Interaction and Ablation Characteristics

Brendan O'Daly
Department of Trauma and Orthopaedic Surgery, Royal College of Surgeons in Ireland, Cappagh National Orthopaedic Hospital, Dublin, Ireland

Edmund Morris
Dublin City University

Graham Gavin
Technological University Dublin, graham.gavin@tudublin.ie

Conor Keane
Department of Pathology, Mater Misercordiae University Hospital, Dublin, Ireland

John O Byrne
Department of Trauma and Orthopaedic Surgery, Royal College of Surgeons in Ireland, Cappagh National Orthopaedic Hospital, Dublin, Ireland

See next page for additional authors

Recommended Citation
O'Daly, B., Morris, E., Gavin, G., O'Keane, C., O'Byrne, J. and G. McGuinness (2011). High Power, Low Frequency Ultrasound: Meniscal Tissue Interaction and Ablation Characteristics. *Ultrasound in Medicine & Biology* Volume 37, Issue 4, April 2011, Pages 556–567. doi:10.1016/j.ultrasmedbio.2011.01.013

HIGH POWER, LOW FREQUENCY ULTRASOUND: MENISCAL TISSUE INTERACTION AND ABLATION CHARACTERISTICS

BRENDAN J. O'DALY, EDMUND MORRIS, **GRAHAM P. GAVIN**, CONOR O'KEANE, JOHN M. O'BYRNE, and GARRETT B. MCGUINNESS

Abstract—This study evaluates high power low frequency ultrasound transmitted *via* a flat vibrating probe tip as an alternative technology for meniscal debridement in the bovine knee. An experimental force controlled testing rig was constructed using a 20 kHz ultrasonic probe suspended vertically from a load cell. Effect of variation in amplitude of distal tip displacement (242–494 μm peak-peak) settings and force (2.5–4.5 N) on tissue removal rate (TRR) and penetration rate (PR) for 52 bovine meniscus samples was analyzed. Temperature elevation in residual meniscus was measured by embedded thermocouples and histologic analysis. As amplitude or force increases, there is a linear increase in TRR (Mean: 0.9 to 11.2 mg/s) and PR (Mean: 0.08 to 0.73 mm/s). Maximum mean temperatures of 84.6°C and 52.3°C were recorded in residual tissue at 2 mm and 4 mm from the ultrasound probe-tissue interface. There is an inverse relationship between both amplitude and force, and temperature elevation, with higher settings resulting in less thermal damage. (E-mail: garrett.mcguinness@dcu.ie)

INTRODUCTION

Powered cutting tools are increasingly used in orthopaedic surgery, in particular in joint arthroscopy. Instruments used for the debridement of degenerative or post-traumatic cartilage and meniscal tears include hand tools, rotary shavers, lasers and radiofrequency ablation probes. The aim of meniscal debridement is to preserve critical knee function in articular congruency, cartilage protection, motion and load distribution, as well as to relieve pain. Operating time, temperature elevation and thermal damage in adjacent tissue have been cited as drawbacks to existing meniscal debridement technologies (Sherk et al. 2002). The effects of morphologic changes on meniscal tissue, knee biomechanics and joint reaction force have not been evaluated. The use of high-power low frequency ultrasound ablation instruments operating in the 20–60 kHz frequency range for this application is appealing since high power, low frequency ultrasound probes are known to fragment both bone and, in combination with suction, soft tissues (Wells 1984; Cimino and Bond 1996). Ultrasonic instruments have not been evaluated either for meniscal debridement, or more generally, for the debridement of hard fibrous tissues. This is despite their continued use as a treatment mainstay for numerous other biologic tissue cutting, fragmentation and removal applications (O'Daly et al. 2008). Potential clinical benefits of this strategy include efficiency, reduced operating time, and reduced temperature generation and thermal damage.

Meniscal tissue is composed of water, proteoglycan and collagen (98% type I collagen), with the collagen fibres arranged in radial, circumferential and axial directions (Fithian et al. 1990). The meniscus behaves in load deformation as a fibre-reinforced porous-permeable composite material, with creep and stress-relaxation behaviour determined by frictional drag caused by fluid flow. The meniscus behaves anisotropically under unconfined compression as a consequence of collagen fibre

orientation in the matrix (Gabrion et al. 2005). Ultrasonic devices are frequently claimed to exhibit the property of "tissue selectivity," which allows them to safely destroy hard tissues, while leaving nearby soft tissues unharmed. The unquantified risk of thermal necrosis in adjacent cartilage and bone, as well as neurologic or vascular damage remains a concern for orthopaedic surgeons and underpins their reticence to use this technology. The objective of the current study is, therefore, to establish the fundamental potential of high power, low frequency ultrasound technology for debridement of fibrous meniscal and cartilaginous tissues. This study will examine the effect of contact between a flat-tipped probe, vibrating at low ultrasonic frequencies (20–60 kHz range), and meniscal tissue samples, separate from any potential effects that could arise from complex tip geometries, or sharp or serrated edges. The intention is to isolate effects due to contact with a surface vibrating at these frequencies from any other modes of cutting or tissue dissection, which might be associated with specific device designs. Experimental evidence of the tissue removal rate, probe penetration rate, temperature effects and histologic damage for a probe relying entirely on ultrasonic vibrations to ablate tissue will establish the intrinsic capability of the technology for debridement of fibrous tissues.

Literature reporting investigations of high-power ultrasonic surgical ablation and tissue failure mode in the frequency range of 20–60 kHz is limited for all tissue types (Wells 1984; Amso 1994). Mechanical aspects of the tissue ablation and damage mechanism are poorly understood and strategies for residual tissue damage minimisation have not been adequately addressed. Where mechanisms of interaction are reported, the available evidence is limited and frequently conflicting. The interaction between ultrasound and living tissue is complex. It depends on the type, condition and composition of tissue, mode of ultrasound application and several acoustic parameters, including frequency, amplitude of vibration, tip area, tip geometry and the resulting pressures or intensities (Cimino and Bond 1996; O'Daly et al. 2008). Few studies have quantified the relative importance of amplitude of vibration, frequency, tip design, suction or target tissue to ultrasonic device performance (Stumpff et al. 1975; Duarte 1983; Chan et al. 1986; Krattiger et al. 1990; Cimino and Bond 1996; Wiksell et al. 2000) and none relate to fibrous meniscal or cartilaginous tissue. Frequency and amplitude of tip displacement are critical factors in the ultrasound tissue interaction and their relative contribution determines the efficiency of tissue fragmentation and degree of residual tissue damage.

Quantification of ultrasonic device efficiency for soft tissue fragmentation, as well as parameters affecting cutting and removal rate, have been examined in experimental studies. Chan et al. (1986) described tissue removal using a 20 kHz ultrasound aspirator in terms of rate per unit time using ox-tissue liver as the test material. Their method permitted examination of the effect on the rate of removal of independently varying frequency, amplitude of vibration and suction pressure. Using a similar quantitative method, Cimino and Bond (1996) identified distal tip peak-to-peak displacement and suction as the two most significant operating parameters affecting rate of fragmentation of visceral tissues. More recently, experimental investigation has focused on quantifying the effect of dissipated ultrasonic energy and resultant damage in residual tissue for individual tissue types. Recent clinical studies have highlighted the deleterious thermal and mechanical effect of ultrasonic energy in residual tissue (Emam and Cuschieri 2003; Koch et al. 2003). Although equivalent experiments have not been performed for harder fibrous tissues, Vangness et al. (2003) have investigated the thermal damage effects of radio-frequency on the human meniscus in a force controlled experimental model. They measured a mean depth of thermal damage in residual tissue of under 2 mm for three commercially available devices operating in the radiofrequency range.

Three modes of interaction are recognised for ultrasound soft tissue interaction. These are (1) direct contact ablation, (2) acoustic effects in the tissues or fluids, including acoustic streaming and cavitation; (3) and thermal effects (NCRP 1983; Cimino and Bond 1996; O'Daly et al. 2008). Combined, they result in shear, fracture and material removal at the tissue surface. Soft tissue removal and damage occurs when a vibrating metal probe is brought into contact with tissue. Energy is concentrated at a narrow tip, resulting in acoustic power densities at the probe-tissue interface that are much higher than that of diagnostic and physical therapy ultrasound devices, with values ranging from 25 to 850 W/cm^2 (Cimino 1999). Ablation and fragmentation effects are seen in tissues in direct contact with the ultrasonic probe and in adjacent tissue over a range believed to be in the order of 0.01–0.1 cm (Carnes and Dunn 1986). The treatment goal is destruction or alteration of tissues in close proximity to the probe tissue interface rather than propagation of vibratory energy in the tissues.

For hard fibrous tissues, interaction and debridement characteristics are not known. No evaluation of the acoustic energy delivered or the mode of interaction has been reported. In contrast to visceral tissue, the efficiency of ultrasonic ablation devices has not been quantified. Little is known about the relative contribution of acoustic parameters to efficacy and damage mechanisms. There is a paucity of studies quantifying microscopic damage in residual tissue (O'Daly et al. 2008). Neither has the range

or area over which clinically relevant deleterious effects occur in these systems been subjected to rigorous investigation.

This study will investigate whether high power low frequency ultrasound transmitted *via* a flat vibrating probe tip can debride and damage hard fibrous meniscal tissue to a degree that would meaningfully assist joint arthroscopy without causing unacceptable levels of damage in residual adjacent tissue.

Aims

The purpose of this study is to explore the resistance of bovine knee meniscus, a fibrous tissue, to ablation by contact with blunt high power, low frequency ultrasound probes. The specific objective of this study, therefore, is to quantitatively investigate the interaction between a high power, low frequency ultrasonic probe and hard, fibrous bovine meniscal tissue, in terms of the influence of vibration amplitude and applied force on tissue removal rate, penetration rate, temperature generation and tissue damage. This study is conducted as a quantitative analysis of the parameters that contribute to this interaction.

MATERIALS AND METHODS

Ultrasonic device

A commercially available acoustic horn connected to an ultrasonic generator was used (Branson Digital Sonifier 450D; Branson Ultrasonics Corporation, Danbury, CT, USA). A 3 mm ultrasonic probe was connected to the acoustic horn (Branson Tapered Microtip 3 mm; Branson Ultrasonics Corporation). The ultrasound probe operated at 20 kHz in continuous (nonpulsatile) mode. Amplitude settings quoted correspond to manufacturer's calibration and are based on total peak-to-peak movement in microns measured on minimum and maximum amplitude settings of the output control. Amplitudes (p-p) of 242 μm, 368 μm and 494 μm correspond to calculated spatial-average-temporal-average intensity values of 312, 720 and 1298 W/cm^2, respectively (Wu and Nyborg 2006).

Force/displacement measurement system

The acoustic horn was suspended vertically from a 500 N load cell (500 N KAP-TC; Angewandte System Technik [AST], Dresden, Germany) in a materials testing machine (Zwick Roell Z005; Zwick Roell GmbH, Ulm, Germany) by means of a rigid holding rig (Fig. 1). The tip of the probe is aligned in the rig so that it moves vertically downwards into the centre of the specimen holding chamber. This arrangement ensures that all load cell forces are applied vertically and perpendicular to the meniscal tissue surface, allowing measurement of downward force by the load cell as the tip of the instrument is placed in contact with the tissue for a range of force and amplitude settings. The load cell is interfaced to computer software and provides a method of direct force

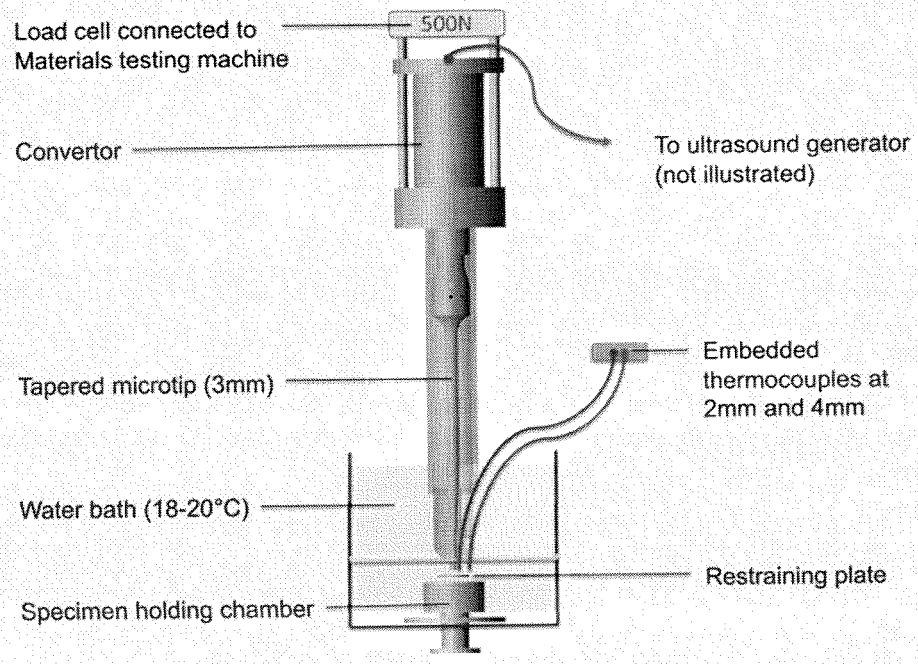

Fig. 1. Experimental rig suspended from 500 N load cell.

measurement applied to the tissue samples by the vibrating ultrasonic probe. The arrangement of the load cell is illustrated in Figure 1. To examine the effect of variations in force on tissue removal rate, for each experiment, a specified starting force is selected (range: 2.5–4.5 N). Starting forces were selected based on measured values for clinicians using an experimental ultrasonic chisel for cutting bone (Khambay and Walmsley 2000). Crosshead starting position is fixed at 1.5 mm above the tissue sample and the force is zero-set. Preliminary experiments were conducted in which the ultrasonically vibrating tip was held at a distance of 1 mm from the surface of the meniscal tissue. For the amplitudes under investigation in this study, no damage to tissue was observed grossly or microscopically in these noncontact experiments.

Test software

The crosshead is interfaced to a computer running TestXpert (v. 11.2) software (Zwick Roell GmbH, Ulm, Germany). The initial displacement of the crosshead to find the predetermined starting force (range: 2.5–4.5 N) is set at 1 mm/s. Load and displacement data are recorded every 0.1 s.

Ultrasound

The ultrasonic generator is started manually for each experiment when the predetermined starting force is reached. The continuous (nonpulsatile) mode is used. The ultrasound generator is switched off when the probe

Meniscal harvesting and storage

Meniscal samples were harvested from bovine knee joints of freshly slaughtered 12 to 15-month-old steer obtained from a local abattoir. All meniscal samples were used within 24–48 h of slaughter. *En bloc* knees were stored at 4°C before experimentation. At the time of experiment, knee joints were disarticulated. Each tibial plateau, with the menisci intact was grossly examined to ensure that there was no damage to the menisci. Menisci were harvested and frozen in 0.15 M (0.9%) NaCl solution with protease inhibitors (N-ethylmalemide, 10 mM; benzamide HCl, 5 mM; ethyldiaminetetraacetic acid, 2 mM; and α-toluenesulphonyl fluoride, 1 mM; (Sigma-Aldrich Inc., St. Louis, MI, USA) and stored in a freezer at –20°C. All specimens were removed from the freezer and allowed to defrost at room temperature for 12 h prior to testing.

Specimen preparation

Uniformly circular meniscal (16 mm) specimens were cut from the meniscus using a 16 mm steel press cutting punch. Specimens were taken from tissue sections located at the avascular region of the meniscus (inner or medial one-third). Distance from the peripheral rim to the most peripheral edge of all specimens was consistently maintained at 25%–40% of meniscal width, to include as little of the vascular zone as possible (Fig. 2). Two surgical blades orientated in parallel (5 mm apart) were used to obtain uniformly thick 5 mm sections from circular meniscus samples. Actual sample thickness was measured using a digital micrometer with three measurements taken for each meniscus and a mean thickness calculated. Specimens were dried with absorbent paper and weighed in a weigh boat using a balance to obtain initial weight. Specimens were removed and placed in 0.15 M NaCl solution with protease inhibitors until testing, to maintain hydration.

Meniscus testing

A raised specimen-holding chamber (16 mm diameter × 5 mm) was placed in a 1500 mL water bath (0.15 M NaCl solution with protease inhibitors) at room temperature. Dimensions of the water bath were 190 mm (w) × 190 mm (l) × 130 mm (h). Temperature in the water bath was maintained at room temperature (18–20°C), to simulate arthroscopic conditions. Meniscal specimens were placed in the specimen holding chamber and a restraining plate placed over the holding chamber and screwed into position, submerged in the saline solution bath (Fig. 3). Meniscal tissue was treated in a reproducible manner according to the force and amplitude settings of the experimental group.

Experimental design

To handle the complexity and difficulty associated with interacting parameters, a response surface methodology (RSM) design was used with both input variables

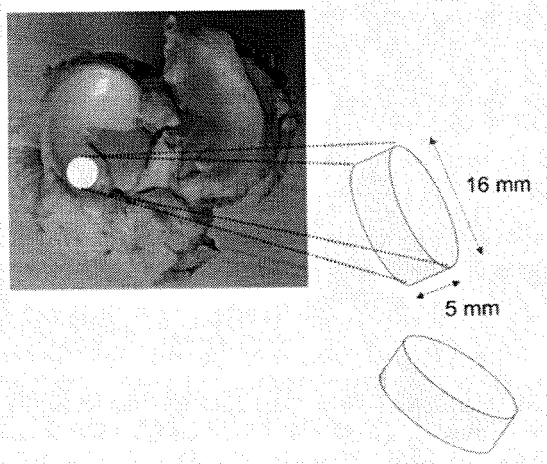

Fig. 2. Meniscal specimen (16 × 5 mm) preparation.

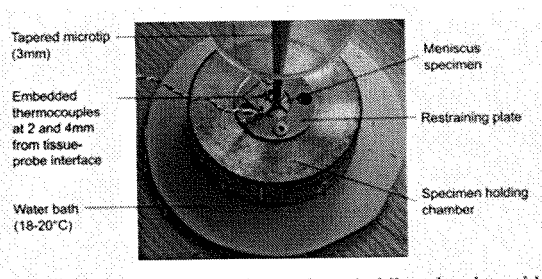

Fig. 3. Meniscal specimens in specimen holding chamber with placement of thermocouples at distances of 2 mm and 4 mm from ultrasonic probe tip. Note cross-hairs to mark centre of meniscal specimen.

(A = amplitude; B = force) treated as continuous (Design-Expert v. 8.0.3, Stat-Ease Inc., Minneapolis, MN, USA). The individual and interactive effects of these (process parameter) variables were studied by conducting the experiment at randomly selected and different levels of both factors (Table 1). A face-centred central composite design ($\alpha = 1$) was selected to avoid testing-machine constraints at low force settings (Montgomery 1997; Montgomery and Runger 1999). This approach selects a limited number of actual experimental combination or "design points," yet provides a statistically relevant assessment of the experiment (Box and Draper 1971; Myers and Montgomery 2002). This method allows probing into possible experimental interaction between parameters studied and their effect on penetration rate, tissue removal rate and temperature generation.

A 13-trial experiment, with eight unique and five replicate trials was used, each with a specified force and amplitude setting. A total of 52 experiments were performed, with four repeat experiments for each force and amplitude setting and their mean value entered in the RSM model.

Input and output variables

Input variables peak-to-peak amplitude of distal tip displacement (μm) and force (N) were examined. Tissue removal rate, penetration rate and temperature at specified locations were the measured output parameters. The time taken for crosshead displacement of 4.5 mm through the tissue specimen was measured. Once the crosshead has travelled this distance, it is withdrawn away from the specimen and returns to its starting point. At the end of the experiment, the specimen is removed from the specimen holding container. The specimen is carefully dried with absorbent paper. Attention is taken not to remove any debris still attached to the specimen. After drying, the specimen is re-weighed (Chan et al. 1986; Cimino and Bond 1996). The difference in weight (Δw) for each specimen before ($w1$) and after ($w2$) ultrasound application is taken as the amount of meniscus removed by the ultrasonic device:

$$\Delta w = w_1 - w_2$$

The tissue removal rate is a time-averaged measurement ($\Delta w/t$). For each experimental trial, this procedure was repeated 10 times. Similarly, penetration rate (mm/s) was calculated as the penetration in mm by the ultrasonic probe, calculated as the difference in position of the crosshead at the start of the experimental trial ($d1$) and the end of the experimental trial ($d2$):

$$\Delta d = d_2 - d_1$$

The penetration rate is a time-averaged measurement ($\Delta d/t$).

Table 1. Levels of process parameters used in the response surface experiment

	Levels		
Process parameter	−1	0	+1
Applied force (N)	2.5	3.5	4.5
Vibration amplitude (p-p) (μm)*	242	368	494

* Amplitude settings quoted correspond to manufacturer's calibration and are based on total peak-to-peak movement in microns measured on minimum and maximum amplitude settings of the output control. (Peak-peak amplitude 242 μm corresponds to setting 3; 368 μm corresponds to setting 5; 494 μm corresponds to setting 7 of Branson Digital Sonifier 450D.)

Temperature measurement

Thermocouples (type K) (T. M. Electronics; Goring, W Sussex, UK) with negative temperature coefficient and exposed junction were used for temperature measurement as a surrogate marker of protein denaturation and tissue necrosis. Two thermocouples were embedded into the 16 mm diameter meniscus samples, at distances of 2 mm and 4 mm from the probe-tissue interface respectively (Fig. 3). Electrical resistance was measured using analogue to digital meters (PicoLog ADC TC-08; Pico Technologies, Cambridgeshire, UK). The meter was interfaced to a computer running Pico Log software (R 5.18.0; Pico Technologies). Graphs were plotted for temperature ($°C$) as a function of time (s).

Calculation of temperature elevation

Temperature elevation was analysed by examining maximum temperatures generated at each thermocouple, as well as the calculation of duration of time during which the temperature was elevated above 40°C for each ultrasound application. This temperature was selected as protein denaturation occurs at a minimum temperature elevation of 4°C above body temperature (Amaral 1994). Necrosis in adjacent bone occurs when temperatures of

45 to 47°C are sustained for periods exceeding 1 min (Goldberg et al. 2005). The area under the curve for which the temperature was greater than 40°C (AUC_{40}) was calculated for each graph of temperature (°C) as a function of time (s) by the formula:

$$AUC_{40}0\_t = \sum_{i=0}^{n-1}(t_{i+1}-t_i)(C_i+C_{i+1})/2$$

Where:

$AUC_{40}0\_t$ = Area under a curve (>40°C for time 0 to t)
t = Time values
C = Temperature >40°C, *e.g.*, C_1 at time t_1, where C represents °C > 40
n = Total number of time temperature points
i = Reference index for i^{th} temperature-time value.

A graphic representation of calculation of AUC_{40} is depicted in Figure 4.

Histologic analysis

For histologic analysis, meniscal specimens were fixed in 10% formaldehyde in a phosphate buffer (pH 7.0 @ 25°C histologic fixative; VWR International Ltd., Lutterworth, UK). Samples were dehydrated in graded series of alcohol and embedded in paraffin. Six-micron (6 μm) sections were cut and stained with hematoxylin and eosin (H&E). Digital Images were captured using the Aperio ScanScope XT Slide Scanner (Aperio Technologies Inc., Vista, CA, USA). A blinded histologic analysis was performed using image analysis microscopy (ImageScope v. 10.0, Aperio Technologies Inc.) by the principal investigator (B.O.'D.) with verification of methods by a consultant pathologist with a musculoskeletal interest (C.O.'K.). The zone of tissue necrosis and zone of thermal alteration were determined by examining the differential staining of the connective tissue and measuring the maximum lateral thermal alteration in tissue adjacent to the cut edges of the meniscal specimen.

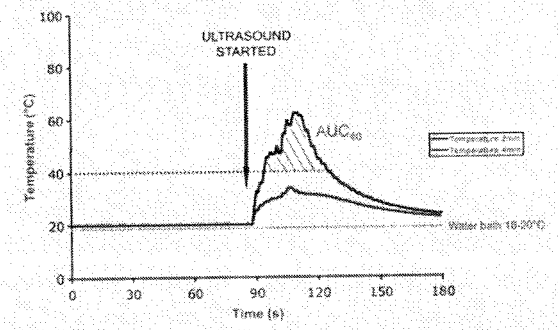

Fig. 4. Graphical representation of calculation of area under the curve for temperatures greater than 40°C (AUC_{40}).

The zone of thermal necrosis was defined as that area of meniscus with collagen denaturation, eosinophilic depigmentation and cell necrosis. The zone of thermal alteration was defined as that area of meniscus with abnormal staining pattern, as compared with control menisci, with only mild alteration of the extracellular matrix (Sherk et al. 1995; Vangsness et al. 1995; Jazrawi et al. 2003). Owing to frequent irregularities in prepared sections and in line with other investigators, a 300 μm zone at the surface of the meniscus and also at the tip of the cut were excluded by drawing two parallel lines to the surface of the meniscus (Plotz et al. 1997). The damaged zone between these two lines was measured as the area of tissue necrosis and alteration on both sides of the cut. The average extent of tissue damage was determined as the area on each side divided by the depth of the zone, and a mean value calculated. Histology sections were prepared for one randomly selected specimen, at each of the 13 trial experiment settings as determined by the RSM design. To investigate the relationship between temperature elevation and thermal damage, depth of thermal necrosis and alteration for each selected specimen were correlated with AUC_{40} 2 mm and AUC_{40} 4 mm data for that individual specimen.

Statistical analysis

Normality was tested using Shapiro–Wilk test. Values for tissue removal rate (mg/s) penetration rate (mm/s) and AUC_{40} (°C.s) are expressed as mean ± standard deviation. A two-way independent between groups analysis of variance (ANOVA) was conducted to explore the impact of input variables (amplitude, force) on output parameters with post-hoc comparison by Tukey's honestly significant difference (HSD) test. Statistical analysis was performed using PASW Statistics (v.18; IBM SPSS Statistics, Chicago, IL, USA). For each response (*e.g.*, tissue removal rate, penetration rate, AUC_{40} 2 mm) all possible models from the mean to sixth-order polynomial were calculated using Design Expert software. Initial model selection was based on: (1) lack of any aliased terms; (2) low residuals; (3) low p value; (4) significant lack of fit; (5) low standard deviation;(6) high R^2, R^2_{adj} and R^2_{pred}; (7) close agreement between R^2_{adj} and R^2_{pred}; and (8) low prediction error sum of squares (PRESS) value in relation to the other models.

The selected model was then further evaluated according to a battery of adequacy tests (Anderson and Whitcomb 2005). Normality was determined by examination of a normal probability plot of the internally studentized residuals and assuring that the residuals fit closely to a straight line. Constant variance was determined by plotting the internally studentized residuals versus the predicted responses. If the points fell within an interval of ±3 standard deviations (σ) and exhibited

a constant range of residuals across the graph, constant variance was assumed. Values for tissue removal rate (g/s), penetration rate (mm/s) and AUC_{40} 2mm (°C.s) are expressed as mean ± standard deviation.

RESULTS

Effect of amplitude and force on tissue removal rate

Large variations in tissue removal rate were observed for different combinations of parameter settings. As amplitude increased (from 242 μm to 494 μm), there was a linear increase in tissue removal rate (range: 0.92 ± 0.41 to 11.16 ± 4.97 mg/s) (Fig. 5a). There was a statistically significant main effect for amplitude [$F(2,42) = 10.24$, $p < 0.001$] (partial eta squared (η^2)= .328) and force [$F(2,42) = 10.97$, $p < 0.001$] ($\eta^2 = .343$). Post-hoc comparisons using the Tukey HSD test indicated that the mean TRR for 242 μm ($M = 1.72$, $SD = 0.89$) p-p amplitude was significantly different from both 368μm ($M = 6.03$, $SD = 3.09$) and 494 μm ($M = 7.06$, $SD = 5.48$) p-p amplitude settings. The mean TRR for 2.5N force ($M = 1.80$, $SD = 1.11$) was significantly different from both 3.5 N ($M = 5.69$, $SD = 3.06$) and 4.5 N ($M = 8.39$, $SD = 5.52$) settings. In addition, the mean TRR for 3.5 N force was significantly different from the mean TRR for 4.5 N. The interaction effect [$F(4,42) = 1.74$, $p = 0.16$] ($\eta^2 = .142$) did not reach statistical significance. The inter-relationship between tissue removal rate, amplitude and force is shown in Figure 5b.

Effect of amplitude and force on penetration rate

A similar correlation between increases in either force or amplitude and increased penetration rate was observed. As amplitude increased (242 μm to 494 μm), we observed a linear increase in penetration rate (range: 0.08 ± 0.04 to 0.73 ± 0.18mm/s) (Fig. 6a). There was a statistically significant main effect for amplitude [$F(2,42) = 33.15$, $p < 0.001$] ($\eta^2 = .612$) and force [$F(2,42) = 22.60$, $p < 0.001$] ($\eta^2 = .518$). Post-hoc comparisons using the Tukey HSD test indicated that the mean PR for 242 μm ($M = 0.12$, $SD = 0.06$) p-p amplitude was significantly different from both 368 μm ($M = 0.40$, $SD = 0.12$) and 494 μm ($M = 0.51$, $SD = 0.28$) p-p amplitude settings. The mean PR for 2.5 N force ($M = 0.16$, $SD = 0.11$) was significantly different from both 3.5 N ($M = 0.40$, $SD = 0.16$) and 4.5 N ($M = 0.52$, $SD = 0.27$) settings. The interaction effect [$F(4,42) = 3.23$, $p = 0.21$] did not reach statistical significance. The relationship between penetration rate, amplitude and force is shown in Figure 6b. From the plot,

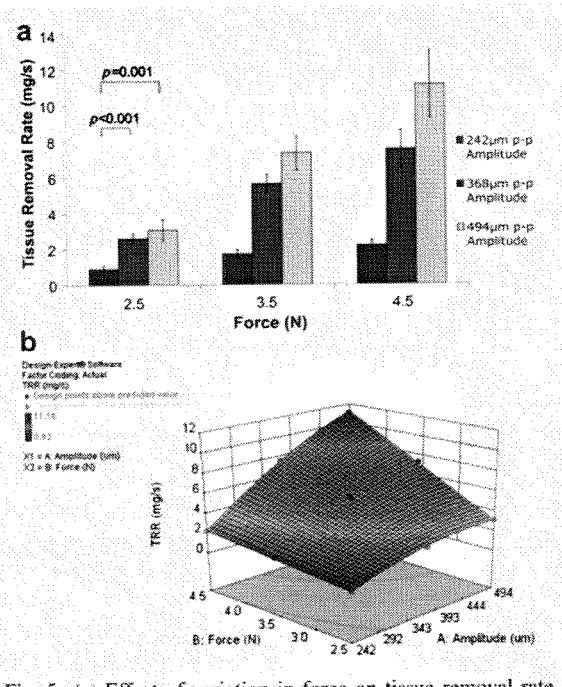

Fig. 5. (a) Effect of variation in force on tissue removal rate (TRR) (mg/s) for p-p amplitude settings 242–494 μm (n = 4). (b) Response surface methodology (RSM) model for tissue removal rate (TRR) (mg/s) for input parameters A = amplitude; B = force.

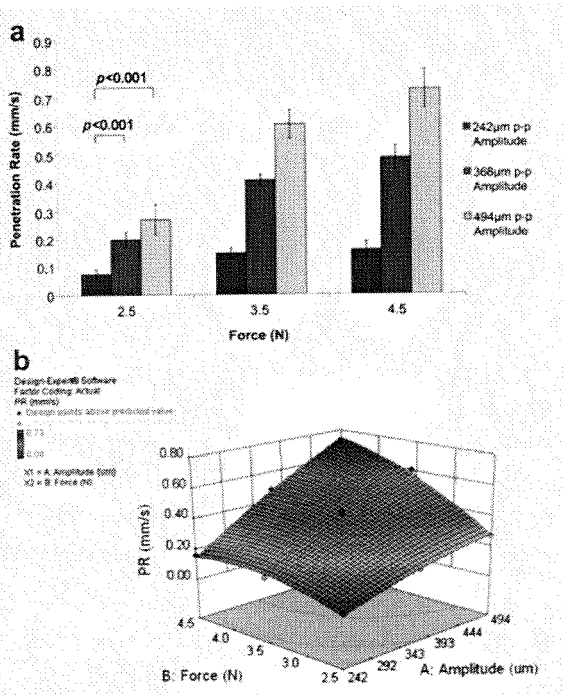

Fig. 6. (a) Effect of variation in force on penetration rate (PR) (mm/s) for p-p amplitude settings 242–494 μm (n = 4). (b) Response surface methodology (RSM) model for penetration rate (PR) (mm/s) for input parameters A = amplitude; B = force.

a penetration rate for any combination of force and amplitude can be obtained.

Temperature measurement

Maximum mean temperatures of 84.6 ± 12.1°C and 52.3 ± 10.9°C were recorded in residual tissue at 2 mm and 4 mm from the probe-tissue interface, respectively. Minimum mean temperatures of 65.9 ± 11.8°C and 39.7 ± 7.1°C were recorded in residual tissue at 2 mm and 4 mm, respectively. Temperature readings greater than 40°C were recorded for 101 s for low amplitude (242 μm) and low force (2.5 N) settings. In contrast for high amplitude (494 μm) and high force (4.5 N) settings, temperature readings greater than 40°C were recorded only for 13 s.

The highest mean value for AUC_{40} of 1754.9 ± 1322.1°C.s was recorded at 2 mm from the probe-tissue interface for amplitude setting 242 μm and force setting of 2.5 N. The lowest mean value for AUC_{40} at 2 mm was 272.7 ± 215.1°C.s, recorded for an amplitude setting 494 μm and force setting of 4.5 N (Fig. 7a). Similarly, at a distance of 4 mm form the probe-tissue interface, the highest mean value for AUC_{40} was 244.6 ± 60.6°C.s. This value was recorded for low amplitude (242 μm) and low force (2.5 N) setting. The lowest mean value for AUC_{40} at 4 mm was 16.0 ± 27.8°C.s, recorded for an amplitude setting 494 μm and force setting of 4.5 N. For AUC_{40} at 2 mm, there was a statistically significant main effect for amplitude [$F(2,41) = 5.71$, $p = 0.006$] ($\eta^2 = .218$). Post-hoc comparisons indicated that the mean AUC_{40} at 2 mm for 242 μm ($M = 1413.04$, $SD = 1114.93$) p-p amplitude was significantly different from that at 494 μm ($M = 541.9$, $SD = 538.9$) p-p amplitude setting. The 368 μm p-p amplitude setting did not differ significantly from either of the other p-p amplitude settings ($M = 720.6$, $SD = 411.1$). For AUC_{40} at 2 mm, the main effect for force [$F(2,41) = 1.33$, $p = 0.42$] and the interaction effect [$F(4,41) = 0.33$, $p = 0.86$] did not reach statistical significance. We found an inverse relationship between both amplitude and force (Fig. 7b) and temperature elevation, with higher amplitude and force settings resulting in less thermal damage in residual tissue at distances of 2 mm from the probe-tissue interface. For AUC_{40} at 4 mm, we found no statistical significant main effect for amplitude, force or their interaction.

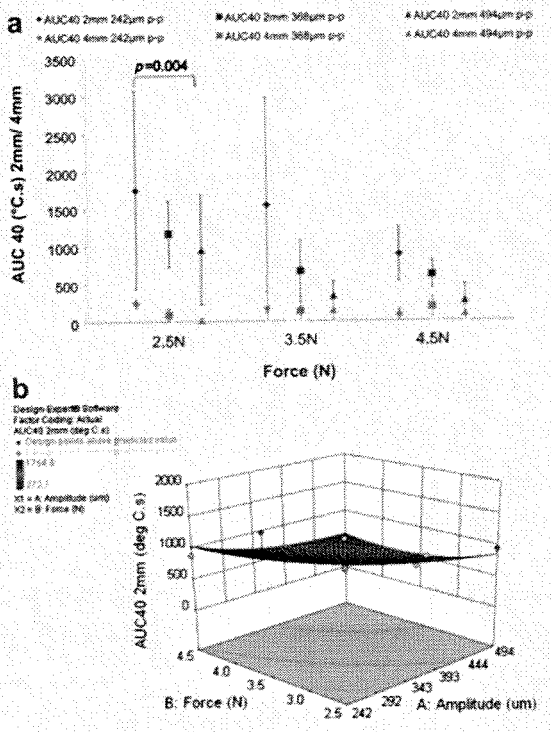

Fig. 7. (a) Effect of variation in force on area under the curve for temperatures greater than 40°C (AUC_{40}) (°C.s) at 2 mm (blue) and 4 mm (orange) from probe-tip interface for p-p amplitude settings 242–494 μm (n = 4). (b) Response surface methodology (RSM) model for area under the curve at 2 mm for temperatures greater than 40°C (AUC_{40}) (°C.s) for input parameters A = amplitude; B = force.

Histologic analysis

The maximum depth of zone of thermal necrosis was 184 μm, recorded for a p-p amplitude setting of 242 μm and a force setting of 3.5 N. The minimum depth of zone of thermal necrosis was 35 μm, recorded for a p-p amplitude setting of 494 μm and a force setting of 4.5 N. The maximum depth of zone of thermal alteration was 787 μm, again recorded for a p-p amplitude setting of 368 μm and a force setting of 3.5 N. The minimum depth of zone of thermal alteration was 177 μm, again recorded for a p-p amplitude setting of 494 μm and a force setting of 4.5 N (Fig. 8). As the selection of specimens for evaluation was random and based on the RSM model, the depths of the zones of thermal alteration and necrosis for each individual specimen has been plotted against the AUC_{40} recording for that sample (Fig. 8). For the central design point (3.5 N, 368 μm), where five repeat trials were performed, the mean depth of zone of thermal alteration was 396 ± 251 μm and the mean depth of the zone of thermal necrosis was 97 ± 44μm. Results were not available for one specimen (settings of 2.5 N force and 494 μm p-p amplitude) that was destroyed during histologic preparation. In general, values recorded for p-p amplitudes of 494 μm show a marked decrease recorded in the depth of the zone of thermal necrosis and zone of thermal alteration when compared with values recorded for 242 μm and 368 μm p-p amplitude settings for equivalent force settings. Histologic images,

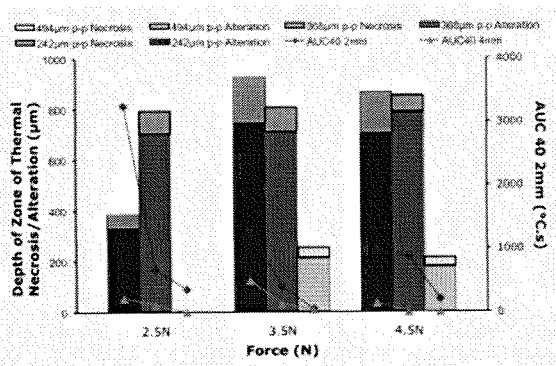

Fig. 8. Effect of variation in force on depth of zone of thermal necrosis (μm) and depth of zone of thermal alteration (μm) for p-p amplitude settings 242–494 μm (bar chart) and comparison with area under the curve for temperatures greater than 40°C (AUC_{40}) (°C.s) at 2 mm (blue line graph) and 4 mm (orange line graph) from probe-tip interface for corresponding specimens at p-p amplitude settings 242–494 μm (n = 1). (Note: specimen for 2.5 N force and 494 μm p-p amplitude destroyed during histologic preparation.)

illustrating the zone of thermal alteration and zone of thermal necrosis are shown in Figure 9.

RSM analysis

Results for experimental and simulated values are listed in Table 2. Output parameters in each experimental run were analyzed using the software and fitted into a multiple nonlinear regression model. The coefficient of the model for the response was estimated using multiple regression analysis technique included in the RSM. The response was measured in terms of tissue removal rate, penetration rate and temperature generation. The quadratic models obtained were given as follows:

$$Y_{TRR}=5.21+2.79X_1+2.38X_2+1.70X_1X_2-0.81X_1^2$$

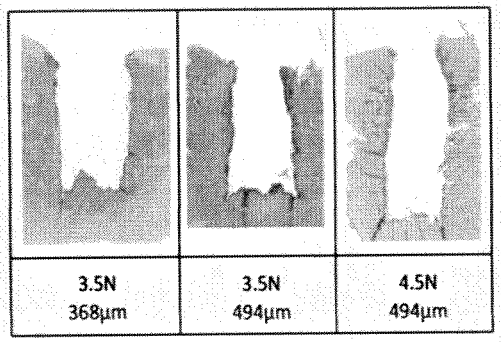

Fig. 9. Histologic tissue specimens (hematoxylin and eosin, H&E; ×5 power) illustrating zone of thermal necrosis and zone of thermal alteration.

X_1 = amplitude and X_2 = force and Y_{TRR} = tissue removal rate

$$Y_{PR}+0.41+0.2X_1+0.14X_2+0.094X_1X_2-0.029X_1^2 -0.067X_2^2$$

Y_{PR} = penetration rate

$$Y_{AUC\ 2mm}=724.87-436.95X_1-350.37X_2+45.58X_1X_2 +161.81X_1^2+111.36X_2^2$$

$Y_{AUC\ 2mm}$ = area under curve (40°C) at 2mm

Accuracy of the model

Analysis of variance (ANOVA) of regression is summarized in Table 3. The maximum predicted responses for optimum settings of applied force and vibration amplitude was obtained through point prediction method and surface response plots. The optimum values of 4.49 N applied force and 493 μm vibration amplitude were determined. These values predict a meniscal TRR of 11.17 mg/s, a PR of 0.74 mm/s, AUC_{40} at 2 mm of 257.3°C.s. The correlation coefficient (R^2) values for the model are high (Table 3). The precision for the chosen model indicates that the signal-to-noise ratio of the data is adequate for these analyses. The coefficient of variation (CV) for this response is low, indicating very close agreement between duplicated measurements in the model.

DISCUSSION

The purpose of this study was a quantitative *in vitro* evaluation of ultrasound efficacy and tissue effects. The intention was to measure tissue removal rate, penetration rate, thermal and damage data on an ultrasound system operating in a controlled setting. In this study, we have shown that for meniscal tissue, responses in tissue removal rate, penetration rate and temperature elevation can be predicted for a force controlled ultrasonic probe on the basis of alterations in user amplitude and force settings. Increases in amplitude and force setting resulted in increased tissue removal rate, increased penetration rate and reduced temperature elevation in adjacent residual meniscal tissue. In addition, this study provides confirmatory evidence of tissue necrosis and tissue alteration occurring at a cellular level in response to temperature elevation. We found that higher amplitude and higher force settings are associated with better performance (increased TRR; increased PR) and reduced temperature elevation and reduced tissue damage. Our findings suggest that an ultrasonic instrument that exploits these operating characteristics may have potential in joint

Table 2. Central composite design with actual and predicted value of output parameters

Run	Amplitude (μm) Code: X_1	Force (N) Code: X_2	Tissue removal rate (mg/s) Actual	Tissue removal rate (mg/s) Predicted	Penetration rate (mm/s) Actual	Penetration rate (mm/s) Predicted	Temperature generation (°C.s) Actual	Temperature generation (°C.s) Predicted
1	242	4.5	2.20	2.23	0.16	0.15	889.2	1039.0
2	368	3.5	5.64	5.27	0.34	0.41	657.6	724.9
3	368	4.5	7.55	7.46	0.48	0.48	619.3	485.9
4	368	3.5	5.06	5.27	0.43	0.41	789.7	724.9
5	368	3.5	4.94	5.27	0.45	0.41	757.4	724.9
6	494	2.5	3.08	3.05	0.27	0.28	956.1	865.9
7	494	3.5	7.35	7.32	0.61	0.58	343.1	449.7
8	368	3.5	5.47	5.27	0.36	0.41	675.9	724.9
9	368	2.5	2.62	2.70	0.20	0.20	1172.4	1186.6
10	494	4.5	11.16	11.22	0.73	0.75	272.70	256.29
11	368	3.5	5.21	5.27	0.44	0.41	624.50	724.87
12	242	2.5	0.92	0.87	0.076	0.061	1754.90	1830.93
13	242	3.5	1.72	1.74	0.15	0.17	1549.50	1323.63

arthroscopy for meniscal and other hard fibrous tissue debridement *in vivo*.

This study employs a flat probe tip design without modification; eliminating artefacts of geometry that might be associated with commercially available probe tips for ultrasonic devices. We did not seek to address how different probe tip geometries might affect performance of an ultrasonic device with these operating parameters. There is no accepted objective means of measurement permitting comparison between individual ultrasonic device control parameters (Cimino 2001). This hinders comparison between individual designs and systems as a basis for interpreting clinical outcomes. With this *in vitro* model, using fresh-frozen meniscal tissue, we attempted to represent the acute mechanical and thermal change that would be seen had the study been performed *in vivo*. The implications of the thermal and histologic changes observed and more specifically, how they might relate to load transmission across the knee is not known.

This study uniquely provides thermal damage data for a fibrous tissue subjected to a high-frequency low-energy ultrasound device. We observed a maximum depth of zone of thermal necrosis of 184 μm and a maximum depth zone of thermal alteration of 787 μm in adjacent residual tissue. Our figures are comparable with reported tissue damage figures for electromagnetic and laser meniscus laboratory surgery. In studies evaluating laser and electrosurgical devices, injury to cartilage and meniscal tissue has been reported, ranging from almost undetectable to 1980 μm in depth (Polousky et al. 2000; Vangsness et al. 2002; King et al. 2005). Additionally, large variations have been reported within experimental groups (Vangsness et al. 2002). The large range of variation in thermal damage among studies may be explained by differences in experimental protocol and by definitions of what constitutes thermal damage. A laboratory study examining the biologic effects of water-borne 25 kHz-ultrasound on murine testicular tissue demonstrated complete absence of thermal damage, instead implicating microstreaming as the physical mechanism of ultrasound-tissue interaction (Carnes and Dunn 1986). Murine testicular tissue is known to have high water content and a low ultrasound absorption coefficient value. In their study, duration of ultrasound exposure, and distance of the ultrasound device from the tissue specimen determined the extent of histologic damage effects. The authors ruled out thermal effects as the source of tissue damage by calculating that temperature elevation in excess of 1°C in testes tissue was not possible using their experimental 15 W/cm^2 intensity ultrasound device. In comparison, we found that the higher spatial-average-temporal-average intensity values of 312–1298 W/cm^2 required for ultrasonic ablation of hard fibrous meniscal tissue result in thermal damage. In a histologic study of fracture healing

Table 3. Analysis of variance of the calculated response surface methodology (RSM) model

	Tissue removal rate (TRR)	Penetration rate (PR)	Temperature generation (AUC_{40} 2mm)
Regression			
Sum of squares	94.56	0.42	2.059×10^6
df	5	5	5
Mean squares	18.91	0.084	4.119×10^5
F value	371.90	50.56	20.7
p value*	<0.0001	<0.001	0.0005
Residual			
Sum of squares	0.36	0.012	1.393×10^5
df	7	7	7
Mean squares	0.051	1.668×10^{-3}	19899.48
Correlation coefficient (R^2)	0.9962	0.9731	0.9366
Coefficient of variation (CV%)	4.66	11.31	16.58

* p value less than 0.0500 indicate model terms are significant.

using low-intensity pulsed ultrasound in bone, Duarte demonstrated a negligible thermal effect, with temperature elevation of less than 0.1°C (Duarte 1983). Results in this study found that ultrasonic energy, with appropriate parameters, can accelerate fracture healing. It is concluded that a nonthermal origin piezoelectric effect is responsible for the stimulation mechanism in hard tissues such as bone. Results in both of these studies are in contrast to our study, which implicates thermal damage as a principal tissue damage mechanism in fibrous meniscal tissue.

Results in this study can be compared with tissue ablation rates reported for visceral tissue (Chan et al. 1986; Cimino and Bond 1996). In common, we found that p-p amplitude of distal tip vibration is an important determinant of tissue removal rate. Rates of removal reported for visceral tissue range from 0 mg/s for aorta, 25 mg/s for liver tissue, to 484 mg/s for brain tissue (Cimino and Bond 1996). In another study using a different device, Chan reported a removal rate of 131 mg/s for liver tissue (Chan et al. 1986). Our maximum rate of 11 mg/s falls within the range reported. Neither of the studies on visceral tissue address thermal or other damage in adjacent residual tissue. In comparison to the current study, neither study attempted to control for applied user force. However, our results demonstrate that alteration in user force significantly affects rate of tissue removal.

There are a number of limitations to our study design. This experiment aimed to standardise meniscal ablation by using an experimental set-up employing a range of forces (2.5–4.5 N) that might be applied manually in a clinical setting. A similar force-controlled experimental set-up has been used by Vangness et al. to study meniscal ablation by radiofrequency ablation (Vangsness et al. 2002). Although it is clear that clinical arthroscopic use involves moving an instrument over the surface of a meniscus, this study employs an ultrasonic probe held in contact with meniscal tissue at a single point for the entire duration of the experiment, potentially exaggerating damage effects in residual tissue. It is highly unlikely that any arthroscopic technique would require holding the instrument in a single position for a prolonged period of time and actual damage in tissue may be less. Studies of bone cutting have shown that if a high temperature is maintained only for very short periods, temperatures in excess of the commonly cited temperature of thermal necrosis will not result in necrosis (Malawer et al. 1999; Lucas et al. 2005). Notwithstanding, we believe that our force controlled experimental design allows maximum control over input parameters and yields useful data that may be applied clinically in instrument design.

We observed large variations in values recorded for AUC_{40} data, with low test-retest reliability between four identical experimental settings at each of 13 trial experiment settings. Variations in time taken for the ultrasound probe to penetrate the tissue sample are primarily responsible for this difference. The observed variation may result from the heterogeneous composition of, and anisotropic response to loading in meniscal tissue samples (Fithian et al. 1990). Others have also reported large variations in thermal damage for meniscal tissue within experimental groups (Miller et al. 1987; Vangsness et al. 2002). The use of AUC_{40} values as a surrogate marker for tissue necrosis and alteration is further questioned by the findings of large differences in values for depth of zone of thermal necrosis and depth of zone of thermal alteration among individual specimens. As only one specimen was tested at each of 13 trial settings, rather than all four and a mean obtained, findings in the current experiment clearly need to be interpreted with caution. Although a general trend toward a reduction in thermal damage at a cellular level is seen with increases in both force and amplitude, it is not apparent why this is not true at the lowest input setting for both parameters, in this experiment (242 μm; 2.5 N). Further work is required to determine what modes of tissue-ultrasound interaction are occurring at each input parameter setting and whether cavitation is occurring at low amplitude settings for this device (Wells 1984).

The results in this study suggest that by judicious control of amplitude and load, it is possible to design an ultrasonic cutting device for meniscal and fibrous tissue debridement that minimizes tissue damage during cutting. This technology warrants further investigation and refinement, to demonstrate equivalence or superiority to current meniscal resection methods.

Acknowledgments—Authors would like to acknowledge funding provided by Enterprise Ireland.

REFERENCES

Amaral JF. The experimental development of an ultrasonically activated scalpel for laparoscopic use. Surg Laparosc Endosc 1994;4:92–99.

Amso NN. Applications of therapeutic ultrasound in medicine. Ultrason Sonochem 1994;1:S69–S71.

Anderson MJ, Whitcomb PJ. RSM simplified: Optimizing processes using response surface methods for design of experiments. New York: Productivity Press; 2005.

Box GEP, Draper NR. Factorial designs, the X'X criterion, and some related matters. Technometrics 1971;13:731–741.

Carnes KI, Dunn F. Low-kilohertz-water-borne ultrasound biological effects. Radiat Environ Biophys 1986;25:235–240.

Chan KK, Watmough DJ, Hope DT, Moir K. A new motor-driven surgical probe and its *in vitro* comparison with the Cavitron ultrasonic surgical aspirator. Ultrasound Med Biol 1986;12:279–283.

Cimino WW. The physics of soft tissue fragmentation using ultrasonic frequency vibration of metal probes. Clin Plast Surg 1999;26: 447–461.

Cimino WW. Ultrasonic surgery: Power quantification and efficiency optimization. Aesthetic Surg J 2001;21:233–241.

Cimino WW, Bond LJ. Physics of ultrasonic surgery using tissue fragmentation: Part I. Ultrasound Med Biol 1996;22:89–100.
Duarte LR. The stimulation of bone growth by ultrasound. Arch Orthop Trauma Surg 1983;101:153–159.
Emam TA, Cuschieri A. How safe is high-power ultrasonic dissection? Ann Surg 2003;237:186–191.
Fithian DC, Kelly MA, Mow VC. Material properties and structure-function relationships in the menisci. Clin Orthop Relat Res 1990; 252:19–31.
Gabrion A, Aimedieu P, Laya Z, Havet E, Mertl P, Grebe R, Laude M. Relationship between ultrastructure and biomechanical properties of the knee meniscus. Surg Radiol Anat 2005;27:507–510.
Goldberg SH, Cohen MS, Young M, Bradnock B. Thermal tissue damage caused by ultrasonic cement removal from the humerus. J Bone Joint Surg Am 2005;87:583–591.
Jazrawi LM, Chen A, Stein D, Heywood CS, Bernstein A, Steiner G, Rokito A. The effects of radiofrequency bipolar thermal energy on human meniscal tissue. Bull Hosp Jt Dis 2003;61:114–117.
Khambay BS, Walmsley AD. Investigations into the use of an ultrasonic chisel to cut bone. Part 1: Forces applied by clinicians. J Dent 2000; 28:31–37.
King JS, Green LM, Bianski BM, Pink MM, Jobe CM. Shaver, bipolar radiofrequency, and saline jet instruments for cutting meniscal tissue: A comparative experimental study on sheep menisci. Arthroscopy 2005;21:844–850.
Koch C, Friedrich T, Metternich F, Tannapfel A, Reimann HP, Eichfeld U. Determination of temperature elevation in tissue during the application of the harmonic scalpel. Ultrasound Med Biol 2003;29:301–309.
Krattiger B, Reinhardt H, Zweifel HJ. [Technical aspects of ultrasound aspiration]. Ultraschall Med 1990;11:81–85.
Lucas M, Cardoni A, MacBeath A. Temperature effects in ultrasonic cutting of natural materials. CIRP Annals 2005;54:195–198.
Malawer MM, Bickels J, Meller I, Buch RG, Henshaw RM, Kollender Y. Cryosurgery in the treatment of giant cell tumor. A long-term follow-up study. Clin Orth Rel Res 1999;359:176–188.
Miller GK, Drennan DB, Maylahn DJ. The effect of technique on histology of arthroscopic partial meniscectomy with electrosurgery. Arthroscopy 1987;3:36–44.
Montgomery DC. Design and analysis of experiments. 4th edition. New York: Wiley; 1997:599–606.
Montgomery DC, Runger GC. Applied statistics and probability for engineers. 2nd edition. New York: Wiley; 1999:705–718.
Myers RH, Montgomery DC. Response surface methodology: Process and product optimization using designed experiments. 2nd edition. New York: Wiley; 2002.
National Council on Radiation Protection and Measurements (NCRP). Biological effects of ultrasound: Mechanisms and clinical implications. Report 74. Bethesda, MD: National Council on Radiation Protection and Measurements; 1983.
O'Daly BJ, Morris E, Gavin GP, O'Byrne JM, McGuinness GB. High-power low-frequency ultrasound: A review of tissue dissection and ablation in medicine and surgery. J Mater Process Tech 2008;200: 38–58.
Plotz W, Fastenmeier K, Burgkart R, Hipp E. Optimization of high-frequency electrosurgery of the meniscus. Knee Surg Sports Traumatol Arthrosc 1997;5:184–188.
Polousky JD, Hedman TP, Vangsness CT Jr. Electrosurgical methods for arthroscopic meniscectomy: A review of the literature. Arthroscopy 2000;16:813–821.
Sherk HH, Black JD, Prodoehl JA, Diven J. The effects of lasers and electrosurgical devices on human meniscal tissue. Clin Orthop Rel Res 1995;310:14–20.
Sherk HH, Vangsness CT, Thabit G III, Jackson RW. Electromagnetic surgical devices in orthopaedics. Lasers and radiofrequency. J Bone Joint Surg Am 2002;8-A:675–681.
Stumpff U, Pohlman R, Trubestein G. A new method to cure thrombi by ultrasonic cavitation. Ultrasonics Intl Conf Proc 1975; 273–275.
Vangsness CT Jr, Akl Y, Nelson SJ, Liaw LH, Smith CF, Marshall GJ. *In vitro* analysis of laser meniscectomy. Clin Orthop Rel Res 1995;310: 21–26.
Vangsness CT Jr, Polousky JD, Hedman TP. Radiofrequency thermal effects on the human meniscus: An *in vitro* analysis. Arthroscopy 2002;18:492–495.
Vangsness CT Jr, Polousky JD, Parkinson AB, Hedman TP. Radiofrequency thermal effects on the human meniscus. An *in vitro* study of systems with monopolar and bipolar electrodes. Am J Sports Med 2003;31:253–256.
Wells PNT. Medical ultrasonics. IEEE Proc A 1984;131:225–232.
Wiksell H, Martin H, Coakham H, Berggren A, Westermark S. Miniaturised ultrasonic aspiration handpiece for increased applicability. Eur J Ultrasound 2000;11:41–46.
Wu J, Nyborg WL. Emerging therapeutic ultrasound. Singapore: World Sientific Publishing Co.; 2006.